

Original Article

Integrative analysis of CBR1 as a prognostic factor associated with IDH-mutant glioblastoma in the Chinese population

Pengxiang Ji*, Xueshi Shan*, Jian Wang, Ping Zhang, Zhan Cai

*Department of Neurosurgery, Suzhou Ruihua Orthopedic Hospital, Suzhou, Jiangsu, China. *Equal contributors*

Received May 15, 2022; Accepted June 22, 2022; Epub August 15, 2022; Published August 30, 2022

Abstract: Background: Glioblastoma multiforme (GBM) is a common primary intracranial tumor with poor prognosis. Common indicators in the clinical diagnosis of glioma include MGMT promoter methylation, isocitrate dehydrogenase (IDH) mutation, 1p/19q codeletion, and TERT mutation. Among these, IDH mutation is extremely important for GBM diagnosis and treatment. Methods: The Chinese Glioma Population Database (CGGA) and Gene Expression Omnibus (GEO) data (GSE131273) related to glioma in the Chinese population were used for differential analysis (DGA) and weighted gene coexpression network analysis (WGCNA). The expression levels of hub genes between the IDH1 wild-type and mutant GBM cell lines were detected by RT-qPCR. Kaplan-Meier (KM) plotter was used to analyze hub gene expression levels and prognostic values. Results: Eight hub genes were identified by WGCNA and different expression genes (DEG) analysis, namely, one upregulated gene (CRYAB) and seven downregulated genes (EFEMP2, RBP1, TAGLN2, CBR1, MSN, ALDH7A1, and MT1M). Four of these genes (ALDH7A1, MSN, CBR1, and MTM1) showed significant differences between IDH-wild-type and IDH-mutant GBM, verified at the cellular level. Moreover, the high expression of CBR1 was significantly correlated with poor overall survival (OS) in patients with IDH-mutant GBM, and we finally identified CBR1 as a specific prognostic factor in IDH-mutant GBM. Conclusion: Results revealed different gene expressions between IDH-wild-type and IDH-mutant GBM. These genes may help monitor the occurrence and development of glioma. CBR1 can be used as a prognostic marker to identify IDH-mutant glioblastoma patients.

Keywords: GBM, IDH mutation, WGCNA, differential analysis, prognostic marker

Introduction

Glioblastoma multiforme (GBM) is a tumor that originates from glial cells and has a high mortality rate [1]. It is also a highly malignant type of glioma. According to the literature reports, the annual incidence of GBM is more than three people per 100,000, and the annual death toll is 30,000 [2, 3]. Considering that glioma typically occurs in the brain, the overall treatment result of glioma is poor. Except for a small number of low-grade glioma patients who can be cured by surgery, most patients with gliomas have poor treatment outcome and are prone to recurrence. Although molecular research on glioma has made substantial progress in the past decade, effective diagnostic and therapeutic approaches are still lacking. There are many reasons for this, such as difficulty in sam-

pling brain tissue, poor permeability of drugs through the blood-brain barrier, redundant intracellular signaling pathways, heterogeneity of tumor molecules, and lack of effective biomarkers. Therefore, it is important to continue to search for diagnostic and treatment markers of GBM and to explore its molecular pathogenesis. Many indicators, such as MGMT promoter methylation, IDH mutation, 1p/19q codeletion, and TERT mutation, have been used in the clinical diagnosis of glioma [4].

IDH is a key enzyme in the tricarboxylic acid cycle that can catalyze the dehydrogenation of isocitrate to α -ketoglutarate (α -KG) [5]. IDH mutations occur through the production of the carcinogenic metabolite D-2-Hydroxyglutarate (D-2HG), which competitively binds with α -KG-dependent enzymes, such as DNA demethylase

TET2 and histone lysine demethylase (KDMs), to prevent lineage specificity [6]. The histone demethylation required for the differentiation of sex progenitor cells into terminally differentiated cells eventually leads to abnormal hypermethylation of DNA and histones, causing abnormal epigenetic modifications and affecting the transcription and expression of certain related genes [7]. IDH1 mutation is the most predominant form. Therefore, finding differential genes in IDH1 mutant GBM will provide a valuable reference for its diagnosis. However, only the study of single gene function level has limited our progress in exploring the mechanism of glioblastoma induction, and further constructing gene networks, analyzing the interaction between genes from the system level will be beneficial to elucidate the mechanism of GBM.

Weighted gene co-expression network analysis (WGCNA) is a representative method for constructing gene co-expression networks [8]. It measures similarity and sets thresholds based on scale-free topology [9]. The method is more reasonable and has been successfully applied to many research fields. WGCNA is a systems biology method to quantitatively measure the degree of interconnection between genes in the network [10]. WGCNA uses topological overlap difference to predict gene modules, which greatly improves the precision of module distinction. At the same time, using topological overlap to describe the relationship of two genes has better stability, reducing the false positive or false negative rate [11]. Therefore, WGCNA is a useful tool to detect gene modules that maintain similar expression patterns of genes.

In the present study, biological information methods, such as WGCNA, were used to identify the differentially expressed genes in GBM after IDH mutation. Results serve as a valuable basis for GBM's molecular diagnosis and treatment.

Materials and methods

Sources of patient information

CGGA database [12, 13] of the Chinese glioma population and the GSE131273 dataset [14] were used to analyze the RNA-seq data of the glioma population by weighted correlation

network analysis (WGCNA). The differentially expressed genes were screened, and the co-expression relationships were grouped together by performing average linkage hierarchical clustering on topological overlap. The clinical data were used for Kaplan-Meier analysis. RNA-seq standardized data from the Cancer Genome Atlas with IDH status and clinical information were downloaded from the Chinese Glioma Population Database CGGA (<http://www.cgga.org.cn>). mRNA microarray data were downloaded from the Chinese Glioma Genome Atlas (CGGA) of diffuse glioma from the GEO Datasets, which also include IDH status and clinical information. The age of onset of the patient was not less than 18 years old. Overall survival (OS) was calculated from the date of diagnosis to death or the end of follow-up.

Data acquisition and processing

First, the DataSet ID of mRNA seq_325 was downloaded from the CGGA website, and the matrix and platform annotation files of the GSE131273 dataset were downloaded based on the "GEO query" of the R software (GPL-23126 [Clariom_D_Human] Affymetrix Human Clariom D Assay [transcript (gene) version]). The gene was reannotated according to the annotation file. Then, the average of the expression levels of the repeated genes in the two data sets was taken. Finally, the "normalize between arrays" function in the R package "limma" was used to normalize the chip expression profile data. In the subsequent analysis, we selected 11 IDH mutant samples and 74 wild-type samples from the CGGA dataset, and 10 IDH mutant samples and 29 wild-type samples from the GSE131273 dataset.

Weighted gene coexpression network analysis (WGCNA)

The CGGA sample cohort was clustered to remove outliers. FPKM>4 was selected, and the shear height was set to 6000. CGGA_1023, CGGA_1320, and CGGA_1275 samples were eliminated. The remaining 82 samples contained 5803 genes. In the GEO analysis, 5369 genes with a mean FPKM>7 were selected for subsequent WGCNA. The shear height was set to 80 to eliminate the three groups of outliers, namely, GSM884999, GSM885028, and GSM884997, thereby leaving 39 groups of samples. The pick soft threshold function was

CBR1 as prognostic factor in IDH-mutant glioblastoma

Table 1. Primers for real-time fluorescent quantitative PCR

Primer name	Sequence
EFEMP2-F	ACAGCTACACGGAATGCACA
EFEMP2-R	TGTAGGTCGTTGATGACGGC
RBP1-F	GCACGCTGAGCACTTTTAGG
RBP1-R	GCTCATCACCCCTCGATCCAC
TAGLN2-F	TCCGCCTTTTCTTTGGCTTTGG
TAGLN2-R	CACATCCTTTTCGGCACTGGGT
CBR1-F	ATAAAACCCCAAGGGAGAGTGG
CBR1-R	TGGTGCACTCCCTTCTTTGTA
MSN-F	CCTACGGGCTGATGCTATGG
MSN-R	GTCGCATGTTCTCAGCATGG
ALDH7A1-F	ATGCACAGATCCGAGTTGGG
ALDH7A1-R	TCCAGGGCGATCCATAACCT
CRYAB-F	AAACATGAAGAGCGCCAGGA
CRYAB-R	TTCACGGGTGATGGGAATGG
MT1M-F	CCTTACCGCGGCTCGAAATG
MT1M-R	GCAGTTCTCCAACGTCCCTTT
ACTB-F	TGTGCGACGAAGACGAGAC
ACTB-R	GACCCATACCGACCATGACG

used to calculate the optimal soft threshold. From the resulting adjacency matrix, we calculated the topological overlap. By using the dynamic hybrid tree cutting algorithm to cut the hierarchical clustering tree and by defining the module as the branch of the cut tree, the modules with similarity values greater than 0.75 were merged [15]. CGGA yielded 15 modules, and GEO analysis yielded 14 sets of gene modules. Finally, we calculated the correlation between the module and the IDH state and selected the two modules most relevant to the mutant in the subsequent analysis.

Taking the intersection of hub genes

We took the DEG analyzed from CGGA and GEO and the genes in the module with the highest correlation with IDH mutant in the WGCNA module, respectively, and made an intersection set. Venn Diagram package of R software was used to show the intersection of four sets of these genes.

Real-time fluorescent quantitative PCR

The reverse transcription system was prepared according to the instructions of the Novizin kit. The reaction product cDNA was placed on ice for subsequent operations or stored at -20°C

(not stored at -80°C for a long time). Real-time fluorescent quantitative PCR was used to detect the mRNA levels of these genes in cells. ACTB was used as an internal reference, and the quantitative primers used were all designed by NCBI (<https://www.ncbi.nlm.nih.gov/>). The primer sequences are shown in **Table 1**.

Cell culture and cell lines

The human glioblastoma cell line U251 was donated by Soochow University. The cells were maintained in DMEM containing 10% fetal bovine serum supplemented with 1% penicillin-streptomycin (10,000 U/ml, Thermo Fisher Scientific). Cells were grown at 37°C in a humidified atmosphere of 5% CO₂ and passaged every 2 days.

Vector construction and transfection

The human IDH1 fragment was cloned into the PCDH vector, and the vector was subjected to site-directed mutation by homologous recombination to convert its encoding of arginine to the encoding of histidine. Digestion was performed with EcoR I and BamH I (Thermo). The lentiviral vector PCDH was digested at the site, and the wild-type and mutant IDH1 fragments were cloned into the vector. The constructed vector was transfected into cells and then screened with puromycin (1 µg/ml) to obtain stable strains overexpressing IDH1-WT and IDH1-MUT.

Western blot analysis

Western blot was used to check expression efficiency. SDS-PAGE was performed on cell lysates. Resolved proteins were electro-transferred onto nitrocellulose membranes (Millipore). Anti-β-actin (Cell Signaling Technology) and anti-HA (Cell Signaling Technology) were added at a 1:1000 dilution and incubated overnight. ECL detection system (Tanon) was used to image.

Statistical analysis

Data were analyzed using R language, SPSS 21.0 software, and GraphPad Prism 7.0 software. Two-tailed t tests were used for differential expression analysis. *P*<0.05 indicates a significant difference. The measured data are expressed as the mean ± SD. The soft thresh-

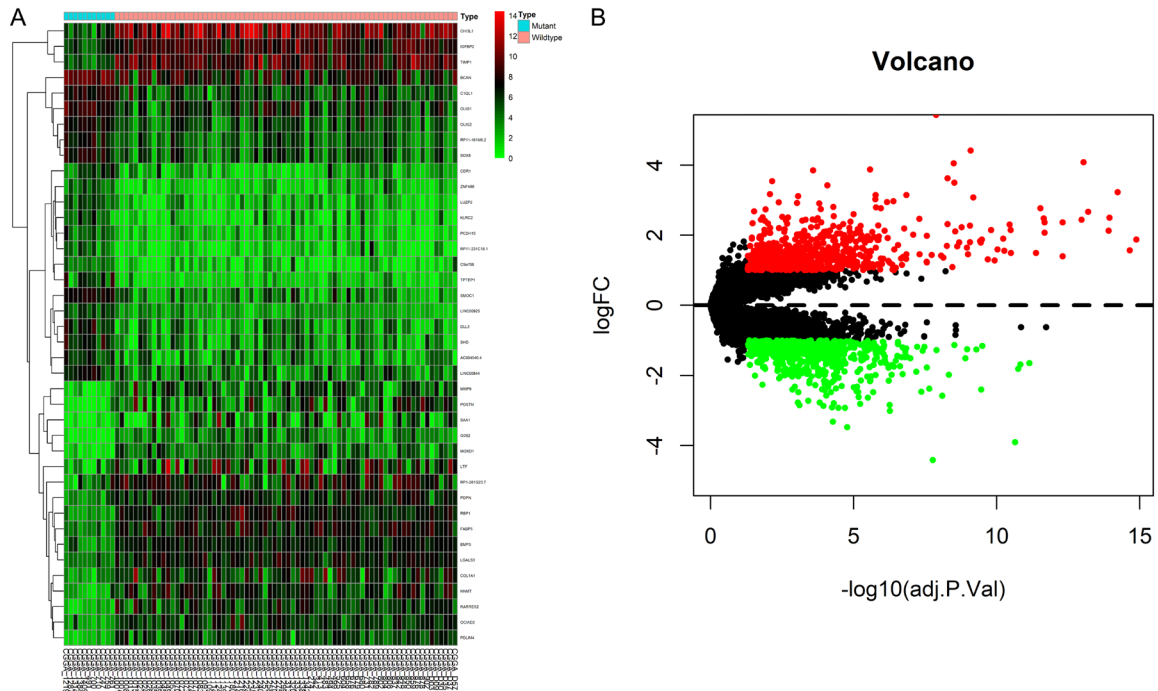


Figure 1. Screening of differentially expressed genes in samples of IDH-mutant GBM patients and IDH wild-type GBM patients in the CGGA dataset; A: Cluster heatmap of heterologously expressed genes (top 20); B: Volcano map of differentially expressed genes; red for upregulated genes and green for downregulated genes, 702 upregulated genes and 593 downregulated genes were obtained.

old of the Pearson correlation matrix was used to determine the strength of the connection between two genes. The Kaplan-Meier estimator and log-rank test were used for univariate survival analysis. Multivariate Cox regression analysis was used to determine independent prognostic factors, and random forest plots were used to analyze IDH classification. * $P < 0.05$, ** $P < 0.01$, and *** $P < 0.001$ are considered significant for all tests.

Results

Screening for differentially expressed genes in the CGGA database

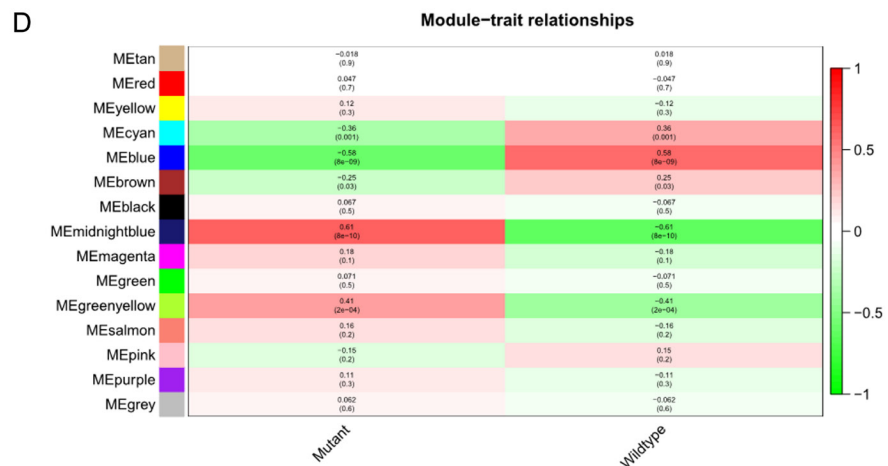
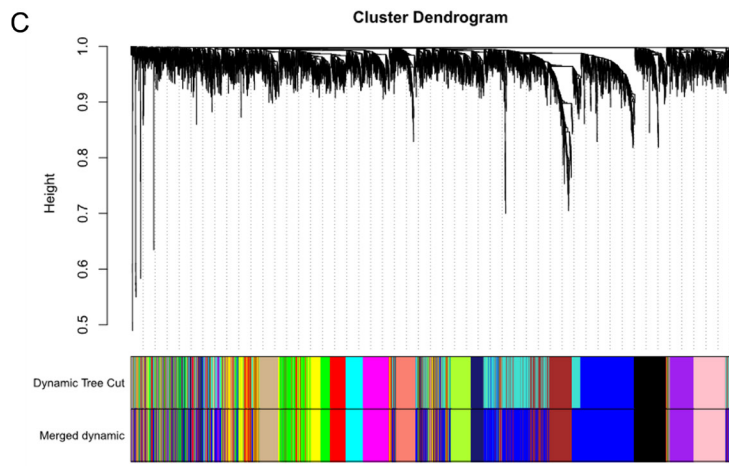
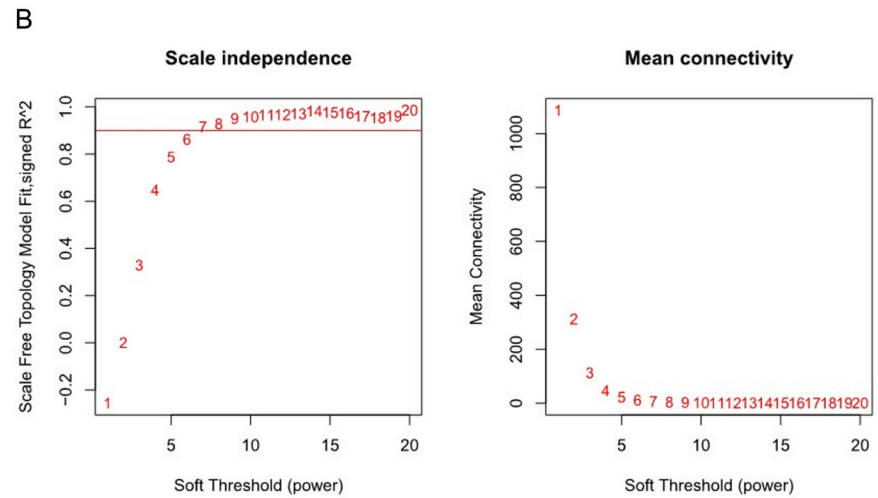
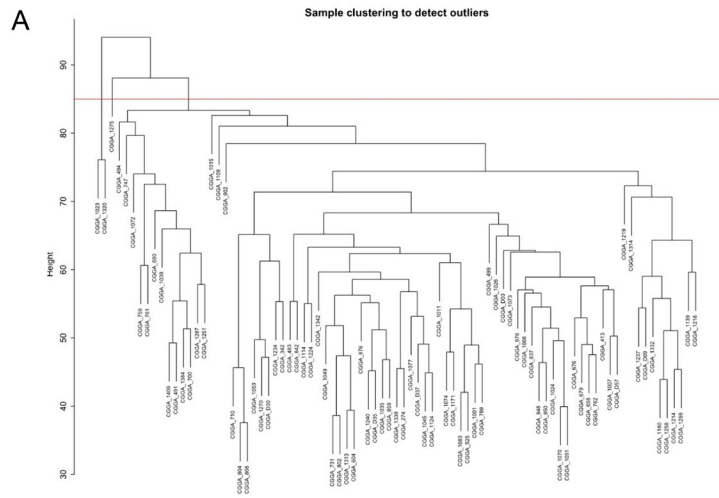
Eighty-five GBM samples were selected from the CGGA database, and the limma package of R software was used to perform difference analysis. The filter conditions were set as $|\logFC| > 1$ and $\text{adj. } P.\text{val} < 0.05$. The correction method used was FDR. The results of DEG analysis were used to construct a volcano map, in which upregulated genes were represented in red, and downregulated genes were represented in green. At the same time, a heatmap was drawn, in which high gene expression levels were denoted in red, and low gene expression

levels were denoted in green (Figure 1A). Each column of the heatmap represented a sample, and each row represented a gene. Similar samples and similar genes were clustered on the abscissa and ordinate, respectively. As a result, 1295 differentially expressed genes were obtained, comprising 702 upregulated genes and 593 downregulated genes (Figure 1B).

Constructing the coexpression module from the CGGA database

GBM samples from the CGGA database were used to screen genes with a mean FPKM > 4 . The shear height was set to 60000, and eight outliers were eliminated (Figure 2A). The optimal soft threshold was set as 7 (Figure 2B), and the minimum gene number in the module was set as 30. The dynamic cutting tree algorithm was used to segment modules and construct a network graph (Figure 2C). As a result, 15 groups of gene modules related to IDH mutations were identified, namely, tan, red, yellow, cyan, blue, brown, black, midnight blue, magenta, green, green yellow, salmon, pink, purple, and gray (Figure 2D). The gray module refers to genes that cannot be clustered to

CBR1 as prognostic factor in IDH-mutant glioblastoma



CBR1 as prognostic factor in IDH-mutant glioblastoma

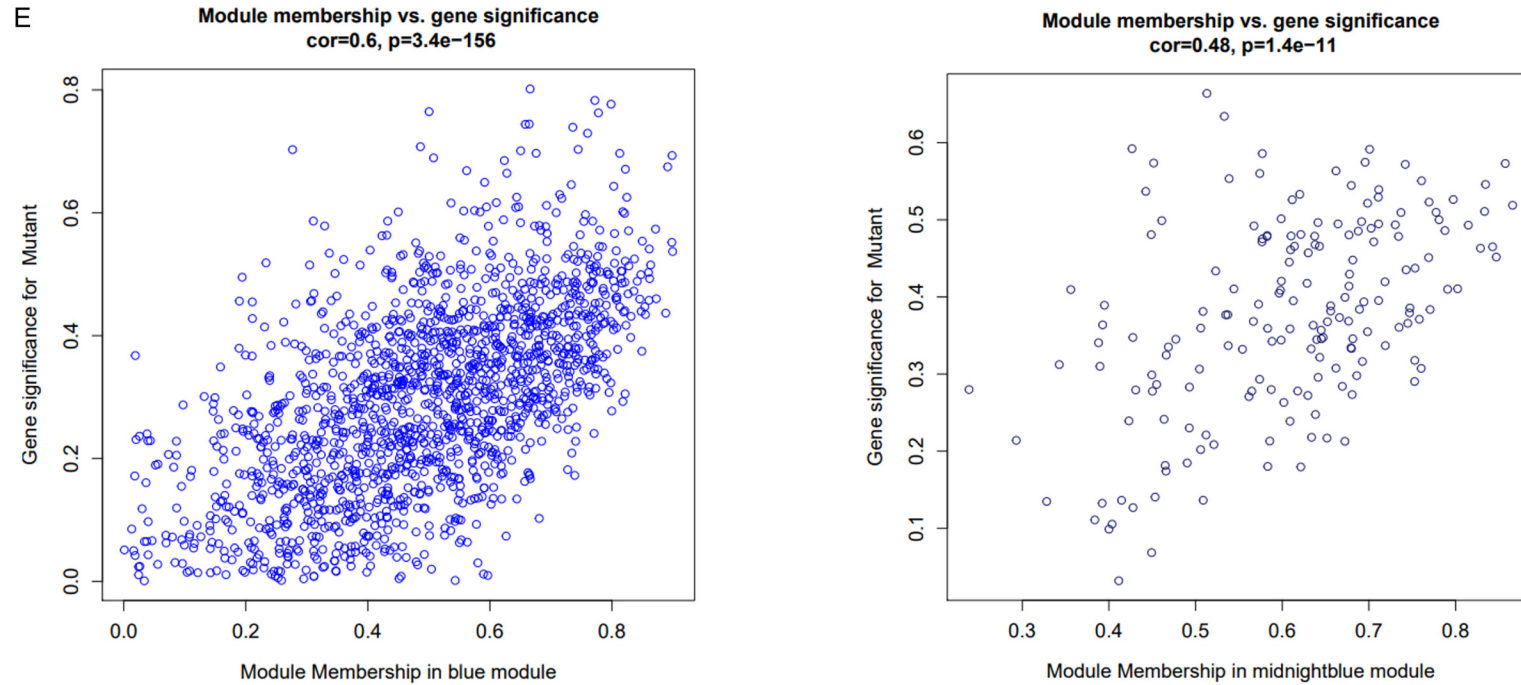


Figure 2. IDH mutation-related coexpression module construction; A: The height is set to 60000 to remove outliers; B: The best soft threshold is determined (in the process of module selection, the adjacency matrix is converted into a topology matrix, and the optimal soft threshold $\beta=7$ is determined); C: Hierarchical data clustering is used to detect coexpression clusters with corresponding color assignments; D: The correlation between gene modules and clinical information is determined (the redder the color is, the higher the correlation is; the numbers in the figure are the Pearson correlation coefficients, and the numbers in parentheses are the corresponding P values); E: GS and MM scatter plots of midnight blue ($cor=0.48, P=1.4e^{-11}$) and blue module genes ($cor=0.6, P=3.4e^{-156}$).

CBR1 as prognostic factor in IDH-mutant glioblastoma

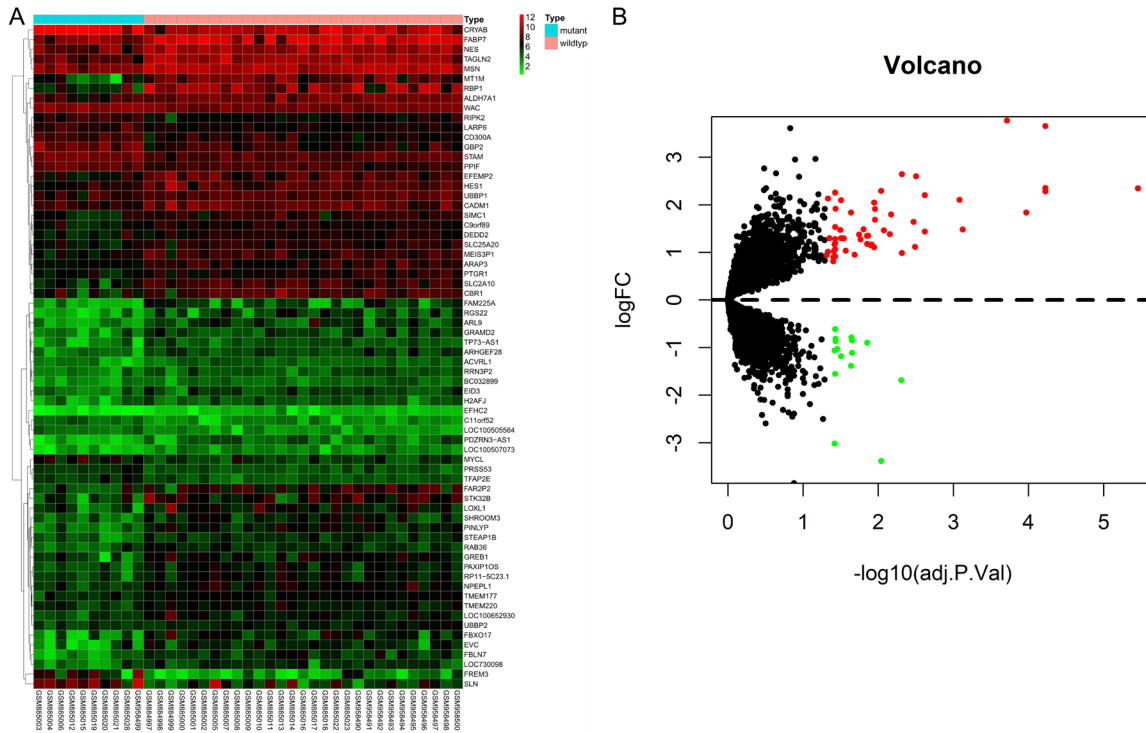


Figure 3. Screening of differential genes in samples of IDH mutant GBM patients and IDH wild-type GBM patients in the 131273 dataset; A: Cluster heatmap of differentially expressed genes; B: Volcano map of differentially expressed genes; red is for upregulated genes, whereas green is for downregulated genes.

other modules. So, it was excluded from subsequent analysis. Then, key modules were identified according to the correlation coefficient between module characteristics and traits. The midnight blue ($cor=0.48$, $P=1.4e^{-11}$) and blue ($cor=0.6$, $P=3.4e^{-156}$) modules had the highest correlation coefficients (Figure 2E).

Screening for differentially expressed genes in GSE131273

We also analyzed the differentially expressed genes between IDH-mutated and wild-type samples in 39 GBM patients in the GSE131273 dataset by the R package Limma. The conditions were set at $|\logFC|>0.5$ and $P<0.05$. Corrected by FDR, $|\logFC|>0.5$ and $P<0.05$ were defined as differentially expressed genes. Thus, there were 53 upregulated genes and 15 downregulated genes (Figure 3).

Constructing the co-expression module from GSE131273

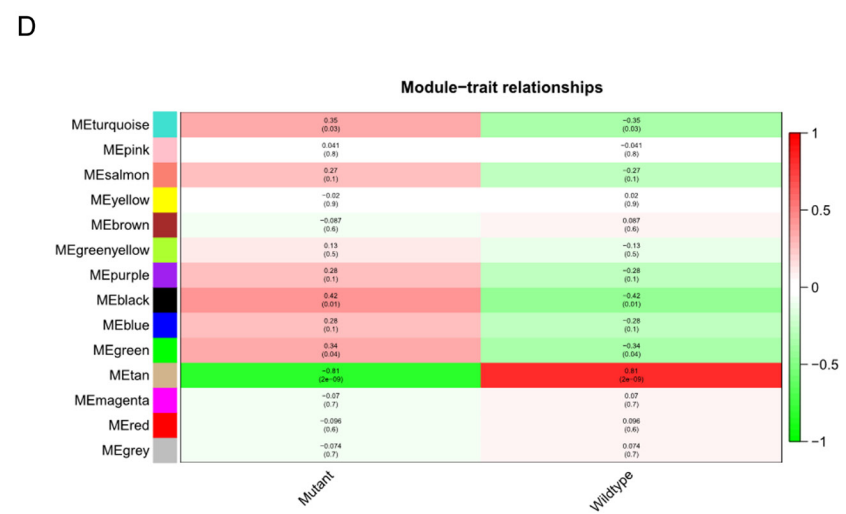
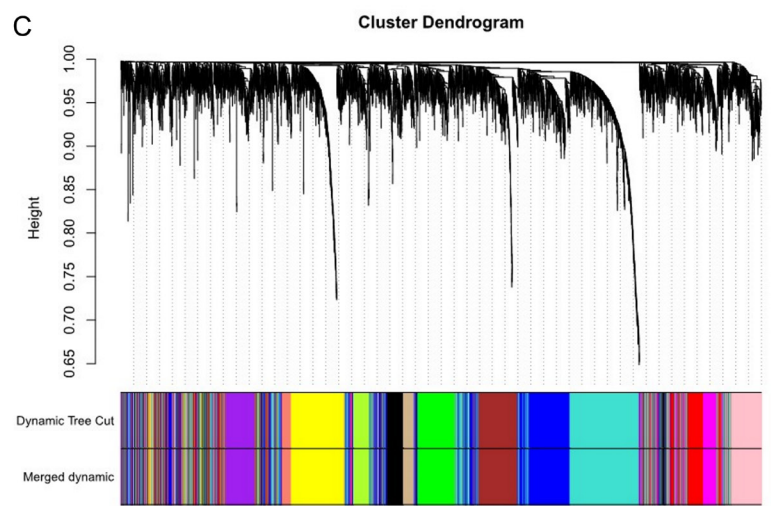
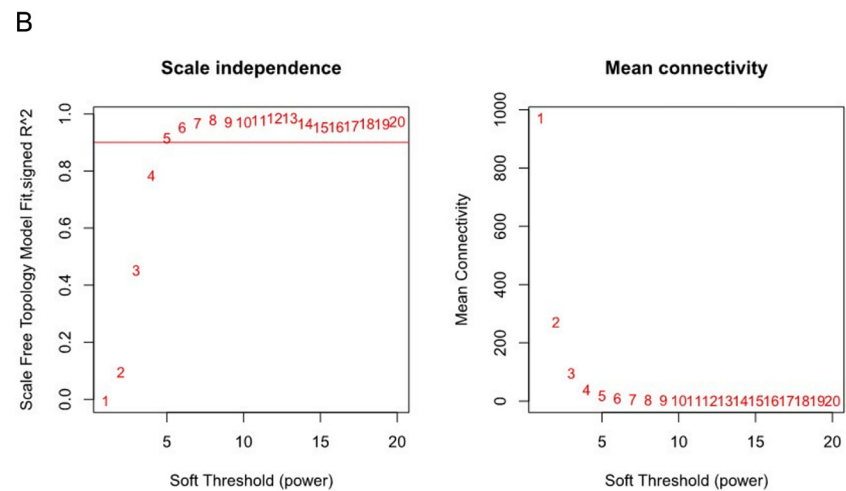
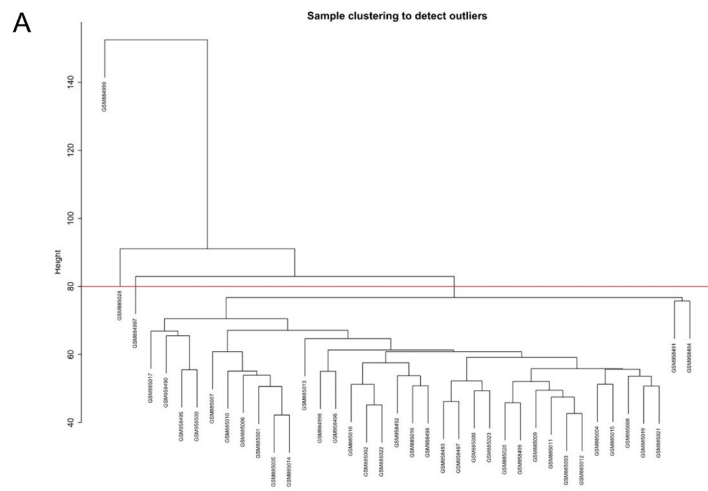
Using RNA chip data U133 Plus 2.0 from the GSE131273 dataset, genes with $FPKM>7$ were selected, and shear height was set to 140 to eliminate one outlier sample (Figure 4A). The

best soft threshold was 5 (Figure 4B), and the smallest gene in the module was 30 (Figure 4C). Fourteen gene modules related to IDH mutations were obtained, namely, turquoise, pink, salmon, yellow, brown, green-yellow, black, blue, green, tan, magenta, red, and gray (Figure 4D). Key modules were also identified according to the correlation coefficient between module characteristics and traits. The black ($cor=0.36$, $P=3.8e^{-10}$) and tan ($cor=0.77$, $P=1.3e^{-33}$) modules had the highest correlation (Figure 4E).

Searching for hub genes

A Venn diagram was drawn using the Venn Diagram package of R software. The Venn diagram consists of four blocks, as follows: the differentially expressed genes in the CGGA data set; and the blue and midnight blue modules that had the highest correlation with IDH mutations in WGCNA. The differentially expressed genes were selected in the GSE131273 dataset, as well as the black and tan modules that were most related to IDH mutations in WGCNA. Finally, eight genes were screened, namely, EFEMP2, RBP1, TAGLN2, CBR1, MSN, ALDH7A1, CRYAB, and MT1M (Figure 5).

CBR1 as prognostic factor in IDH-mutant glioblastoma



CBR1 as prognostic factor in IDH-mutant glioblastoma

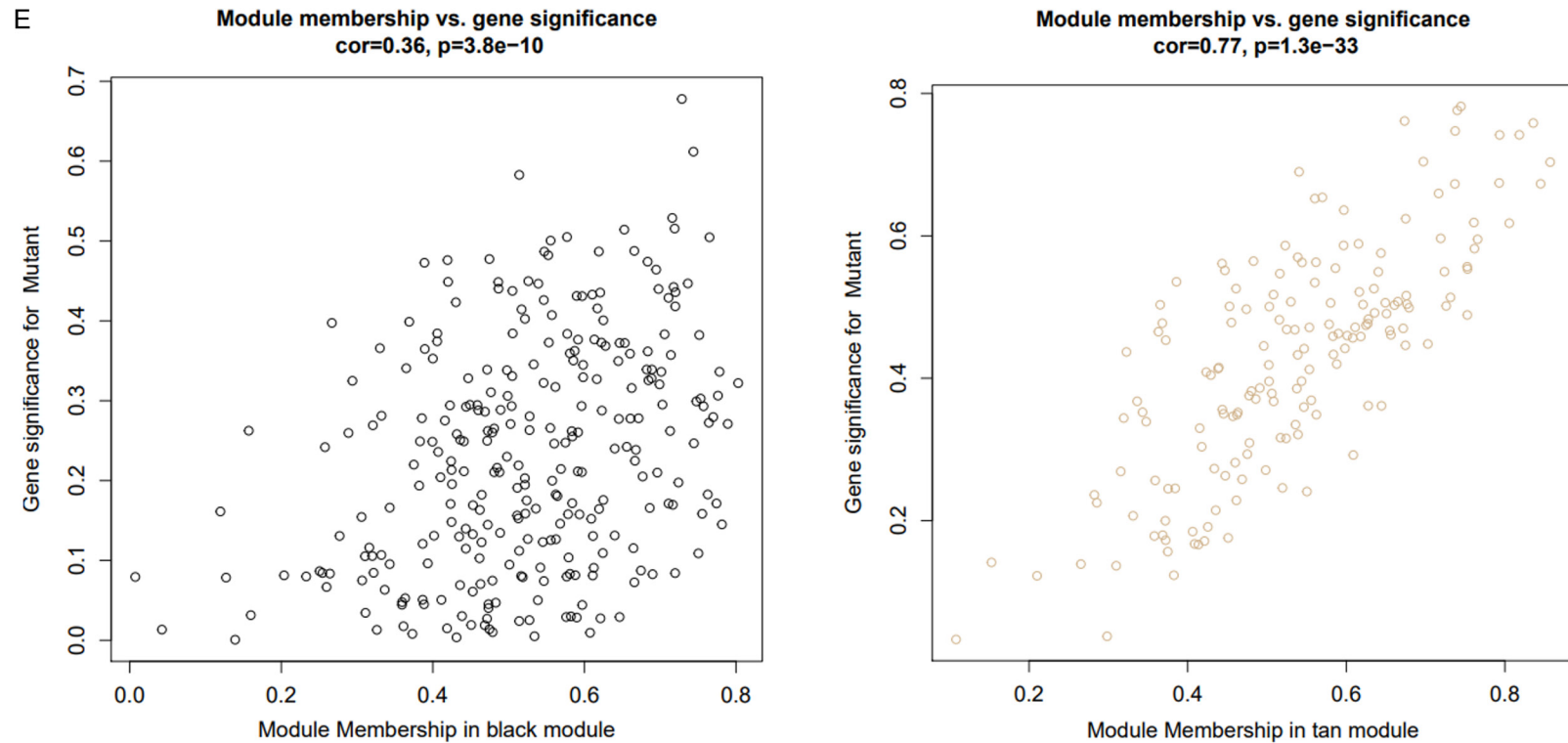


Figure 4. Construction of IDH mutation-related coexpression modules; A: The height is set to 140 to remove outliers; B: The best soft threshold is determined (in the process of module selection, the adjacency matrix is converted into a topology matrix, and the optimal soft threshold $\beta=5$ is determined); C: Hierarchical data clustering is used to detect coexpression clusters with corresponding color assignments; D: The correlation between gene modules and clinical information is determined (the redder the color is, the higher the correlation is; the numbers in the figure are Pearson correlation coefficients, and the numbers in parentheses are the corresponding P values); E: GS and MM scatter plots of black (cor=0.36, $P=3.8e^{-10}$) and tan module genes (cor=0.77, $P=1.3e^{-33}$).

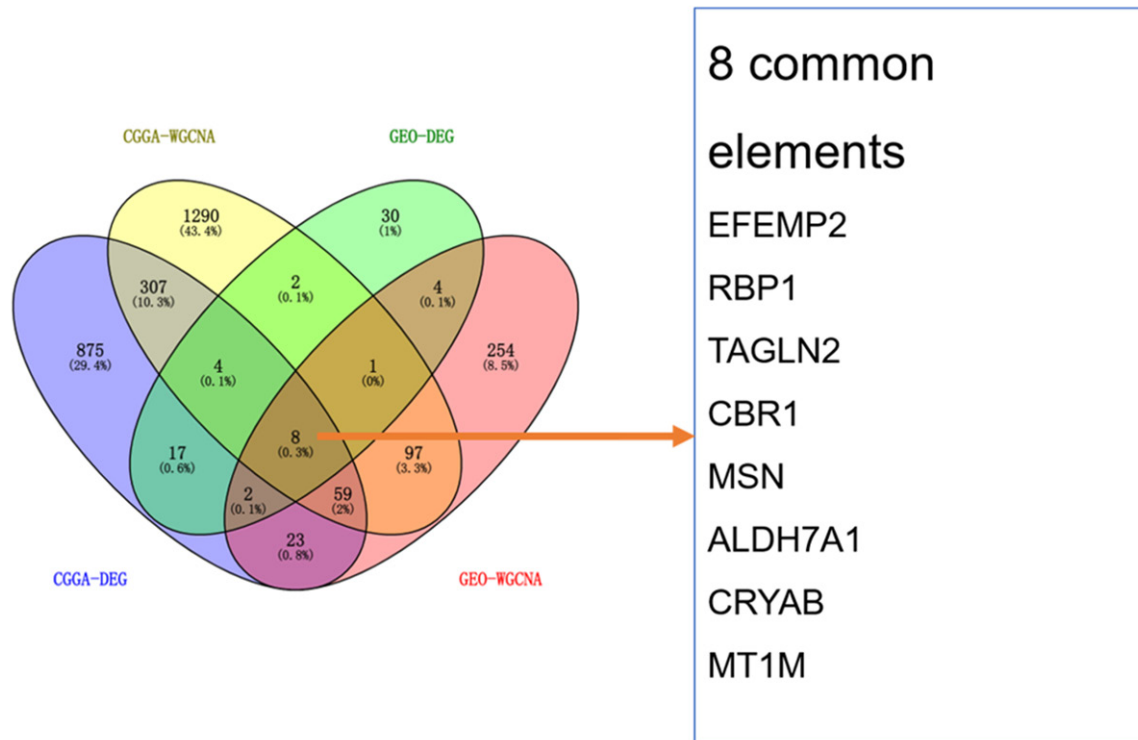


Figure 5. The Venn Diagram package of R software is used to draw a Venn diagram to intersect the above results, EFEMP2, RBP1, TAGLN2, CBR1, MSN, ALDH7A1, CRYAB, and MT1M were screened.

Validating the key genes at the cellular level

The most common mutation in the IDH1 gene occurs at the 132nd arginine residue (R132H and 88%). So, we constructed plasmids containing IDH1 and IDH1-R132H and transfected the two plasmids into the U251 glioblastoma cell line (**Figure 6A**). Western blot was used to detect the expression levels of wild-type and mutant IDH1 proteins in U251 cells (**Figure 6B**). RNA was extracted, and real-time qPCR was used to detect the mRNA expression levels of these eight genes. Four genes (ALDH7A1, MSN, CBR1, and MTM1) were significantly different between wild-type and IDH mutant cells ($P < 0.05$), suggesting that these genes can be used as biomarkers of glioblastoma (**Figure 6C**).

CBR1 can be a prognostic marker for IDH-mutant GBM

To further evaluate the association of the above four genes (ALDH7A1, MSN, CBR1, and MTM1) with the survival rate of glioma patients, we used Kaplan-Meier analysis to determine the relationship between these genes and prognosis of glioma patients with different malignan-

cies (all types, WHO grade II, WHO grade III, and WHO IV; GBM is WHO IV) and IDH status (wild or mutated). We first performed a survival analysis of all primary gliomas and found that high expression of these genes was associated with poor prognosis. However, when we narrowed the detection to IDH-mutant GBM, the other three genes lost significant prognostic value (**Figure S1**) and only CBR1 was evident in IDH-mutant GBM. Interestingly, CBR1 was not significantly correlated with WHO grade II, WHO grade III, and IDH-wt GBM. However, in IDH-mutant glioblastoma, CBR1 expression was significantly negatively correlated with prognosis ($P=0.001$). This result indicated that CBR1 can be used as an IDH-specific molecular marker for mutant glioblastoma. CBR1 may serve as an important reference for the prognosis of gliomas, especially in IDH-mutant GBM (**Figure 7**).

Discussion

Glioblastomas are among the most common malignant tumors in the human central nervous system and seriously endanger health. They are closely related to biological, genomic, inflammatory, and metabolic factors. While previous

CBR1 as prognostic factor in IDH-mutant glioblastoma

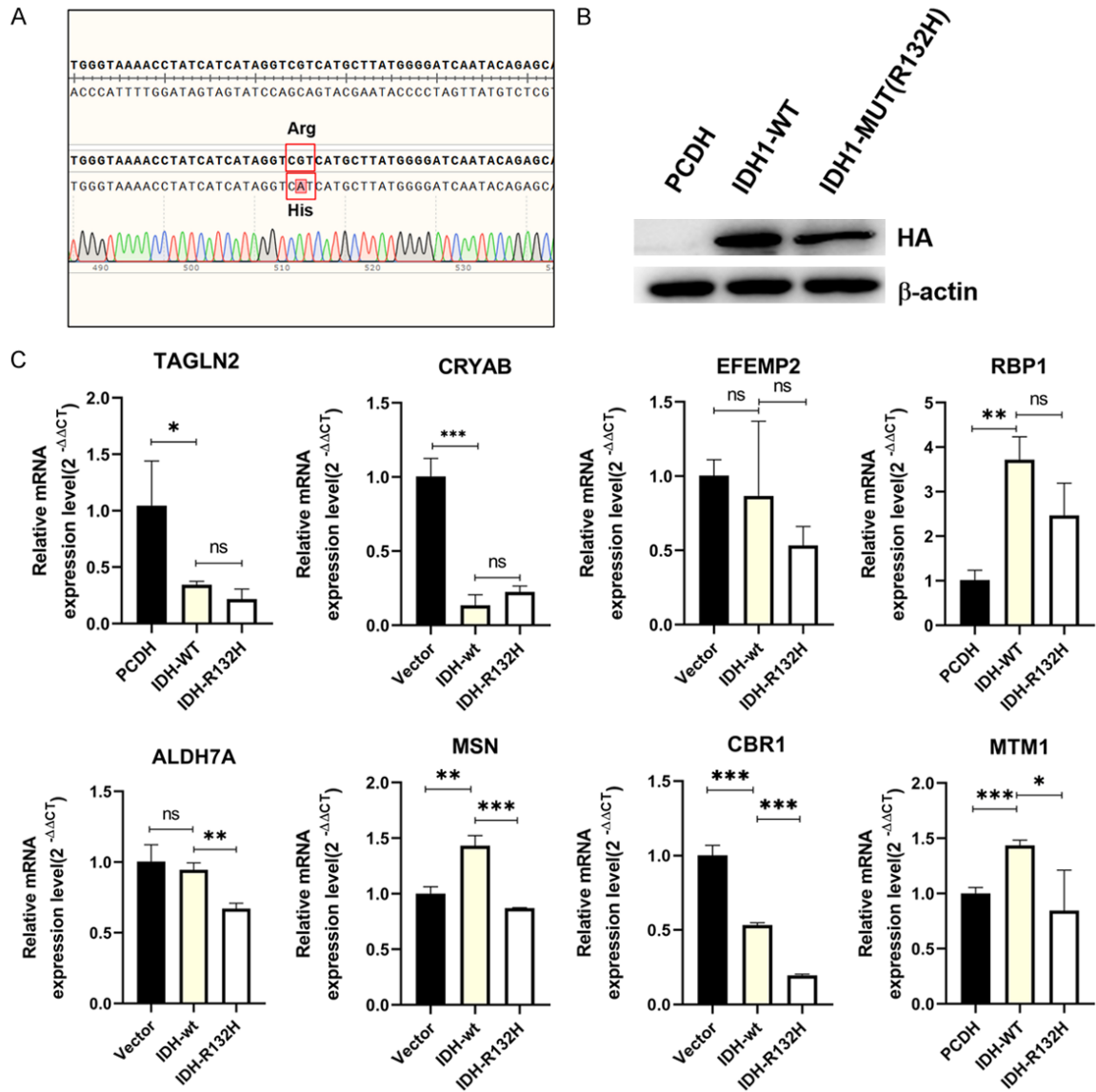


Figure 6. IDH wild-type and mutant GBM cells were constructed, and RT-qPCR was used to detect the mRNA levels of different genes. A: Sequencing results of wild-type and mutant IDH1 vectors; B: Western blot (see Figure S2) is used to detect the IDH1 expression levels of stable strains; C: RT-qPCR is used to detect mRNA levels of EFEMP2, RBP1, TAGLN2, CBR1, MSN, CRYAB, and MTM1 (* $P < 0.05$, ** $P < 0.01$, and *** $P < 0.001$).

identification of isocitrate dehydrogenase (IDH) gene mutations occurred in a small proportion of gliomas, this has changed our understanding of glioma biology, genomics, and metabolism. IDH mutations are mainly found in three types of IDH molecules, namely, IDH1, IDH2, and IDH3. The IDH1 mutation is the most common. It accounts for 80% of all IDH mutations, and the main form of this molecule is the mutation of arginine at position 132 to histidine (R132H) [17, 18]. IDH mutations are related to the metabolic processes of glucose, lipids, and amino acids in both physiologic and pathologic pro-

cesses [19, 20]. IDH mutations are a double-edged sword in gliomas. On the one hand, the production of 2-HG can inhibit the activity of TET enzymes, thereby hypermethylating the promoter regions of some tumor suppressor genes [21]. On the other hand, IDH mutations will bring more targets for the treatment of gliomas, which greatly improves the clinical prognosis.

Current studies have shown that IDH mutation is an important molecular marker for glioma typing and has important biological significance

CBR1 as prognostic factor in IDH-mutant glioblastoma

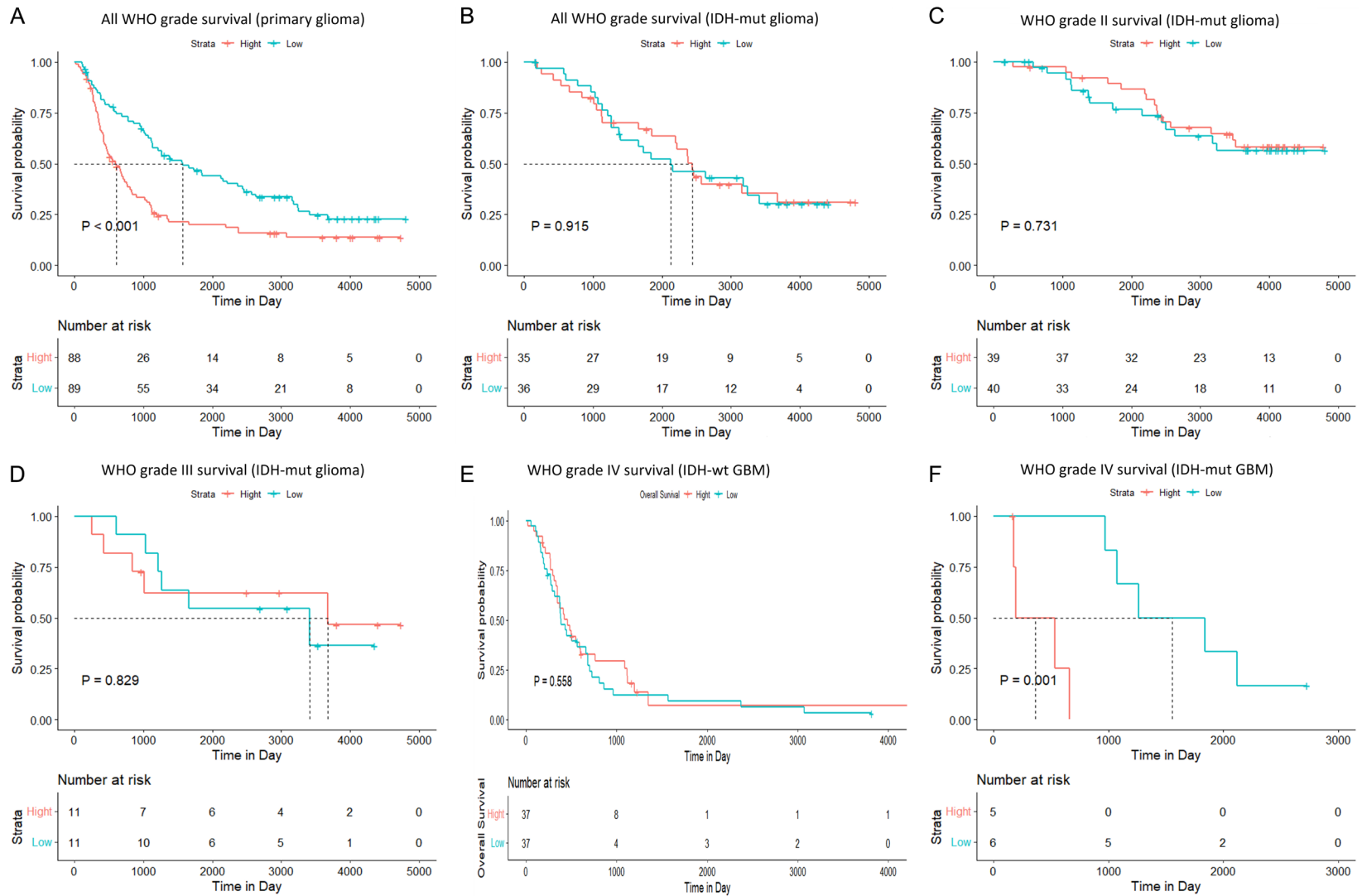


Figure 7. Kaplan-Meier survival analysis of CBR1 in different types of gliomas. A: Survival analysis of CBR1 in primary gliomas of all WHO grades ($P < 0.001$); B: Survival analysis of CBR1 in IDH-mutant gliomas of all WHO grades ($P = 0.915$); C: Survival analysis of CBR1 in WHO grade II gliomas ($P = 0.731$); D: Survival analysis of CBR1 in WHO grade III gliomas ($P = 0.829$); E: Survival analysis of CBR1 in IDH-wild-type GBM ($P = 0.558$); F: Survival analysis of CBR1 in IDH-mutant GBM ($P = 0.001$).

for the prognosis and treatment of glioma. We identified differentially expressed genes associated with IDH mutants, analyzed the transcriptome data of the Chinese glioblastoma population in the CGGA database and GSE dataset using WGCNA, and found the presence of significantly different genes in IDH mutant gliomas. To further clarify the diagnostic value of these genes, we verified the glioblastoma cell line U251 by RT-qPCR and finally obtained four differentially expressed genes: ALDH7A1, MTM1, MSN, and CBR1. Among them, ALDH7A1 is a member of subfamily seven of the aldehyde dehydrogenase gene family [22], which plays a major role in the detoxification of aldehydes produced by alcohol metabolism and lipid peroxidation [23]. MSNs can promote the occurrence, development, invasion, and metastasis of gliomas [24]. MTM1 encodes a dual-specific phosphatase that acts on both phosphotyrosine and phosphoserine [25]. It is related to muscle-related diseases and has not been studied in detail in GBM [26].

Carbonyl reductase 1 (CBR1) is an NADP-dependent enzyme associated with detoxification; it catalyzes the conversion of carbonyl-containing compounds. CBR1 has been reported to act on adducts between glutathione and lipid peroxidation-derived aldehydes [27]. Carbonyl reductase 1 (CBR1) has different functions in different tumors [28]. In head and neck squamous cell carcinoma, CBR1 can promote catenin-mediated epithelial-mesenchymal transition by reducing ROS [29]. In ovarian cancer, this gene can promote tumor proliferation, invasion, and metastasis, but it is rarely reported in glioma.

CBR1 is a key factor that efficiently catalyzes the reduction of glutathionylated aldehydes derived from lipid peroxidation and may play a vital role in the complex metabolic processes of gliomas [30]. We found that CBR1 was differentially expressed in IDH-wild-type and IDH-mutant glioblastomas by WGCNA and validated the differential expression of CBR-1 at the cellular level by qPCR. By Kaplan-Meier analysis, we also found that high expression of CBR1 is not conducive to the prognosis of gliomas, especially in IDH-mutant GBM. This result provides a valuable reference for the diagnosis and prognosis of IDH-mutant glioma and may become a new target for comprehensive glioma treatment.

However, this study has some limitations. Due to the small number of IDH-mutant samples, it is impossible to represent all IDH-mutant GBM patients. In the future, we will further explore the data related to IDH-mutant GBM and their survival information. Using the conclusions of this paper, we will conduct further clinical validation of these genes and carry out relevant experiments to verify their molecular mechanisms in the occurrence and development of gliomas. At the same time, we will also investigate what signaling pathways are these genes associated with. This will provide effective diagnostic and therapeutic targets for IDH-mutant gliomas in clinical medicine.

Acknowledgements

This study was supported by grants from Suzhou Municipal Science and Technology Bureau (SKJYD2021033, SKJY2021022, and SYSD2020052), Suzhou, China.

Disclosure of conflict of interest

None.

Address correspondence to: Ping Zhang and Zhan Cai, Department of Neurosurgery, Suzhou Ruihua Orthopedic Hospital, Suzhou 215104, Jiangsu, China. E-mail: zhangping825@163.com (PZ); pxcz@sina.com (ZC)

References

- [1] Oliveira AI, Anjo SI, Vieira de Castro J, Serra SC, Salgado AJ, Manadas B and Costa BM. Cross-talk between glial and glioblastoma cells triggers the “go-or-grow” phenotype of tumor cells. *Cell Commun Signal* 2017; 15: 37.
- [2] Witthayanuwat S, Pesee M, Supaadirek C, Supakalin N, Thamronganantasakul K and Krusun S. Survival analysis of glioblastoma multiforme. *Asian Pac J Cancer Prev* 2018; 19: 2613-2617.
- [3] Chen J, Tong X, Han M, Zhao S, Ji L, Qin Y, He Z, Pan Y, Wang C and Liu A. Cost-effectiveness of short-course radiation plus temozolomide for the treatment of newly diagnosed glioblastoma among elderly patients in china and the united states. *Front Pharmacol* 2021; 12: 743979.
- [4] Eckel-Passow JE, Lachance DH, Molinaro AM, Walsh KM, Decker PA, Sicotte H, Pekmezci M, Rice T, Kosel ML, Smirnov IV, Sarkar G, Caron AA, Kollmeyer TM, Praska CE, Chada AR, Halder C, Hansen HM, McCoy LS, Bracci PM, Mar-

CBR1 as prognostic factor in IDH-mutant glioblastoma

- shall R, Zheng S, Reis GF, Pico AR, O'Neill BP, Buckner JC, Giannini C, Huse JT, Perry A, Tihan T, Berger MS, Chang SM, Prados MD, Wiemels J, Wiencke JK, Wrensch MR and Jenkins RB. Glioma groups based on 1p/19q, IDH, and TERT promoter mutations in tumors. *N Engl J Med* 2015; 372: 2499-2508.
- [5] Guo J, Zhang R, Yang Z, Duan Z, Yin D and Zhou Y. Biological roles and therapeutic applications of IDH2 mutations in human cancer. *Front Oncol* 2021; 11: 644857.
- [6] Flavahan WA, Drier Y, Liau BB, Gillespie SM, Venteicher AS, Stemmer-Rachamimov AO, Suva ML and Bernstein BE. Insulator dysfunction and oncogene activation in IDH mutant gliomas. *Nature* 2016; 529: 110-114.
- [7] Reiter-Brennan C, Semmler L and Klein A. The effects of 2-hydroxyglutarate on the tumorigenesis of gliomas. *Contemp Oncol (Pozn)* 2018; 22: 215-222.
- [8] Pei G, Chen L and Zhang W. WGCNA application to proteomic and metabolomic data analysis. *Methods Enzymol* 2017; 585: 135-158.
- [9] Back M, Yurdagul A Jr, Tabas I, Oorni K and Kovanen PT. Inflammation and its resolution in atherosclerosis: mediators and therapeutic opportunities. *Nat Rev Cardiol* 2019; 16: 389-406.
- [10] Cao M, Li L, Xu L, Fang M, Xing X, Zhou C, Ren W, Wang L and Jing F. STAT1: a novel candidate biomarker and potential therapeutic target of the recurrent aphthous stomatitis. *BMC Oral Health* 2021; 21: 524.
- [11] Shuai M, He D and Chen X. Optimizing weighted gene co-expression network analysis with a multi-threaded calculation of the topological overlap matrix. *Stat Appl Genet Mol Biol* 2021; 20: 145-153.
- [12] Oldrini B, Vaquero-Siguero N, Mu Q, Kroon P, Zhang Y, Galan-Ganga M, Bao Z, Wang Z, Liu H, Sa JK, Zhao J, Kim H, Rodriguez-Perales S, Nam DH, Verhaak RGW, Rabadan R, Jiang T, Wang J and Squatrito M. MGMT genomic rearrangements contribute to chemotherapy resistance in gliomas. *Nat Commun* 2020; 11: 3883.
- [13] Zhao Z, Zhang KN, Wang Q, Li G, Zeng F, Zhang Y, Wu F, Chai R, Wang Z, Zhang C, Zhang W, Bao Z and Jiang T. Chinese Glioma Genome Atlas (CGGA): a comprehensive resource with functional genomic data from chinese glioma patients. *Genomics Proteomics Bioinformatics* 2021; 19: 1-12.
- [14] Li J, Xue Y, Wenger A, Sun Y, Wang Z, Zhang C, Zhang Y, Fekete B, Rydenhag B, Jakola AS, Jiang T, Caren H and Fan X. Individual assignment of adult diffuse gliomas into the EM/PM molecular subtypes using a taqman low-density array. *Clin Cancer Res* 2019; 25: 7068-7077.
- [15] Li XT. Identification of key genes for laryngeal squamous cell carcinoma using weighted co-expression network analysis. *Oncol Lett* 2016; 11: 3327-3331.
- [16] Horbinski C, Kelly L, Nikiforov YE, Durso MB and Nikiforova MN. Detection of IDH1 and IDH2 mutations by fluorescence melting curve analysis as a diagnostic tool for brain biopsies. *J Mol Diagn* 2010; 12: 487-492.
- [17] May JL, Kouri FM, Hurley LA, Liu J, Tommasini-Ghelfi S, Ji Y, Gao P, Calvert AE, Lee A, Chandel NS, Davuluri RV, Horbinski CM, Locasale JW and Stegh AH. IDH3alpha regulates one-carbon metabolism in glioblastoma. *Sci Adv* 2019; 5: eaat0456.
- [18] Krell D, Assoku M, Galloway M, Mulholland P, Tomlinson I and Bardella C. Screen for IDH1, IDH2, IDH3, D2HGDH and L2HGDH mutations in glioblastoma. *PLoS One* 2011; 6: e19868.
- [19] Liu X, Yamaguchi K, Takane K, Zhu C, Hirata M, Hikiba Y, Maeda S, Furukawa Y and Ikenoue T. Cancer-associated IDH mutations induce Glut1 expression and glucose metabolic disorders through a PI3K/Akt/mTORC1-Hif1alpha axis. *PLoS One* 2021; 16: e0257090.
- [20] Nakae S, Murayama K, Sasaki H, Kumon M, Nishiyama Y, Ohba S, Adachi K, Nagahisa S, Hayashi T, Inamasu J, Abe M, Hasegawa M and Hirose Y. Prediction of genetic subgroups in adult supra tentorial gliomas by pre- and intraoperative parameters. *J Neurooncol* 2017; 131: 403-412.
- [21] Xu Q, Wang K, Wang L, Zhu Y, Zhou G, Xie D and Yang Q. IDH1/2 mutants inhibit TET-promoted oxidation of RNA 5mC to 5hmC. *PLoS One* 2016; 11: e0161261.
- [22] Coughlin CR 2nd, Tseng LA, Abdenur JE, Ashmore C, Boemer F, Bok LA, Boyer M, Buhas D, Clayton PT, Das A, Dekker H, Evangeliou A, Feillet F, Footitt EJ, Gospe SM Jr, Hartmann H, Kara M, Kristensen E, Lee J, Lilje R, Longo N, Lunsing RJ, Mills P, Papadopoulou MT, Pearl PL, Piazzon F, Plecko B, Saini AG, Santra S, Sjarif DR, Stockler-Ipsiroglu S, Striano P, Van Hove JLK, Verhoeven-Duif NM, Wijburg FA, Zuberi SM and van Karnebeek CDM. Consensus guidelines for the diagnosis and management of pyridoxine-dependent epilepsy due to alpha-aminoacidic semialdehyde dehydrogenase deficiency. *J Inher Metab Dis* 2021; 44: 178-192.
- [23] Korasick DA and Tanner JJ. Impact of missense mutations in the ALDH7A1 gene on enzyme structure and catalytic function. *Biochimie* 2021; 183: 49-54.
- [24] Qin Y, Chen W, Liu B, Zhou L, Deng L, Niu W, Bao D, Cheng C, Li D, Liu S and Niu C. MiR-200c inhibits the tumor progression of glioma via targeting moesin. *Theranostics* 2017; 7: 1663-1673.

CBR1 as prognostic factor in IDH-mutant glioblastoma

- [25] Kutchukian C, Szentesi P, Allard B, Buj-Bello A, Csernoch L and Jacquemond V. Ca(2+)-induced sarcoplasmic reticulum Ca(2+) release in myotubularin-deficient muscle fibers. *Cell Calcium* 2019; 80: 91-100.
- [26] Al-Qusairi L, Prokic I, Amoasii L, Kretz C, Messaddeq N, Mandel JL and Laporte J. Lack of myotubularin (MTM1) leads to muscle hypotrophy through unbalanced regulation of the autophagy and ubiquitin-proteasome pathways. *FASEB J* 2013; 27: 3384-3394.
- [27] Barracco V, Moschini R, Renzone G, Cappiello M, Balestri F, Scaloni A, Mura U and Del-Corso A. Dehydrogenase/reductase activity of human carbonyl reductase 1 with NADP(H) acting as a prosthetic group. *Biochem Biophys Res Commun* 2020; 522: 259-263.
- [28] Zhou L, Yang C, Zhong W, Wang Q, Zhang D, Zhang J, Xie S and Xu M. Chrysin induces autophagy-dependent ferroptosis to increase chemosensitivity to gemcitabine by targeting CBR1 in pancreatic cancer cells. *Biochem Pharmacol* 2021; 193: 114813.
- [29] Zhou S, Cao H, Zhao Y, Li X, Zhang J, Hou C, Ma Y and Wang Q. RACK1 promotes hepatocellular carcinoma cell survival via CBR1 by suppressing TNF-alpha-induced ROS generation. *Oncol Lett* 2016; 12: 5303-5308.
- [30] Moschini R, Rotondo R, Renzone G, Balestri F, Cappiello M, Scaloni A, Mura U and Del-Corso A. Kinetic features of carbonyl reductase 1 acting on glutathionylated aldehydes. *Chem Biol Interact* 2017; 276: 127-132.

CBR1 as prognostic factor in IDH-mutant glioblastoma

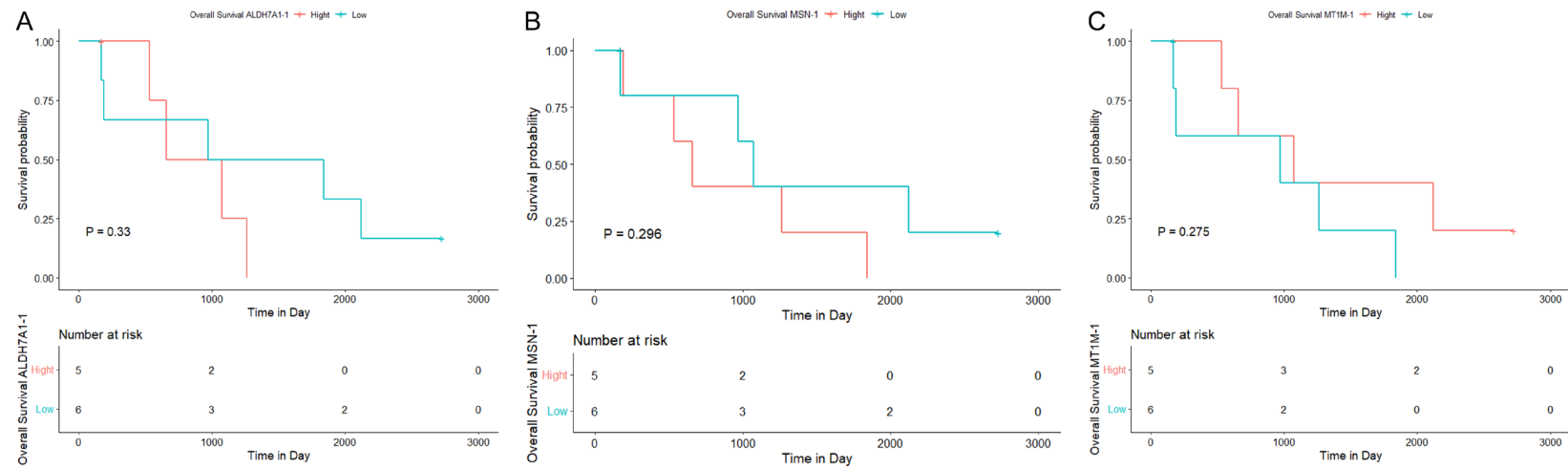


Figure S1. Kaplan-Meier survival analysis of the other three genes in IDH-mutant GBM; A. Survival analysis of ALDH7A1 in IDH-mutant GBM (P=0.33); B. Survival analysis of MSN in IDH-mutant GBM (P=0.296); C. Survival analysis of MTM1 in IDH-mutant GBM (P=0.276).

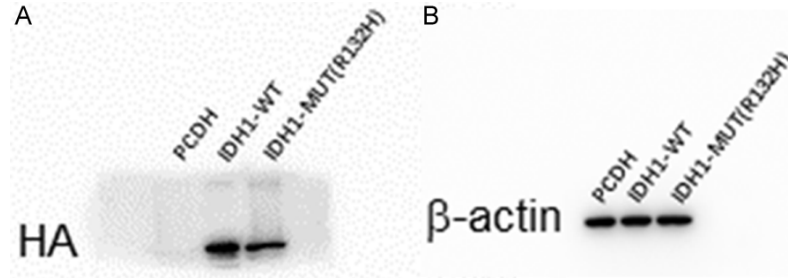


Figure S2. Full-length western blot images; A. Expression of HA-IDH1 (wt/mut) detected by western blot; B. Expression of β -actin detected by western blot.